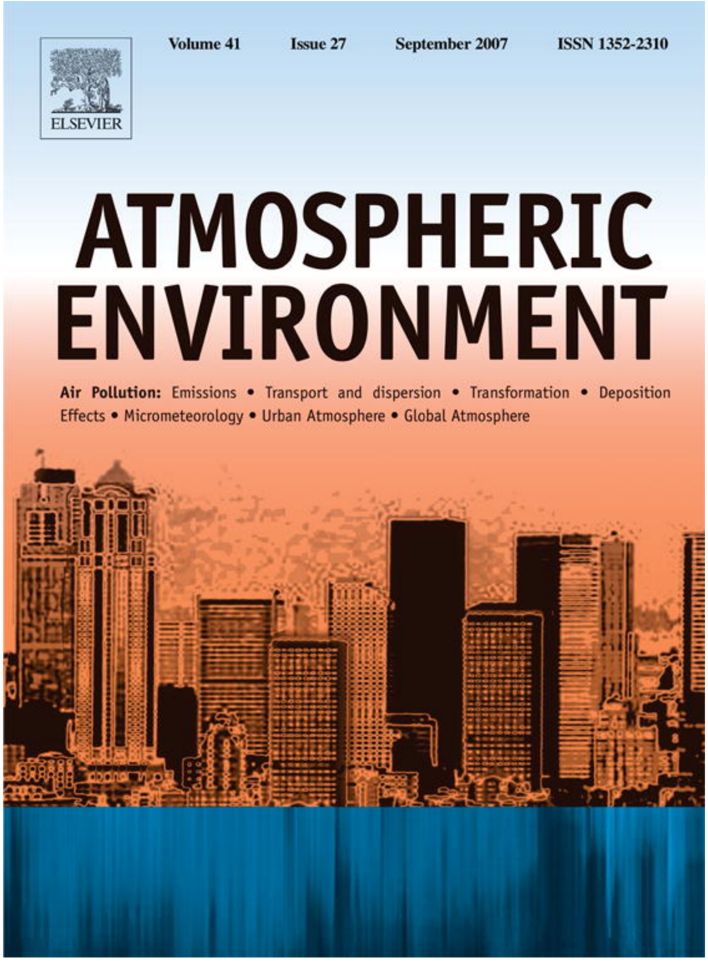
Volume 41
Issue 27
September 2007
ISSN 1352-2310
ELSEVIER
ATMOSPHERIC ENVIRONMENT
Air Pollution: Emissions • Transport and dispersion • Transformation • Deposition
Effects • Micrometeorology • Urban Atmosphere • Global Atmosphere

Available online at www.sciencedirect.com
ScienceDirect
Atmospheric Environment 41 (2007) 5732–5745
ATMOSPHERIC ENVIRONMENT
www.elsevier.com/locate/atmosenv

Validation of the integrated RAMS-Hg modelling system using wet deposition observations for eastern North America

Antigoni Voudouri, George Kallos*

School of Physics, Atmospheric Modelling and Weather Forecasting Group, University of Athens, University Campus, Bldg Phys-V, Athens 15784, Greece

Received 17 June 2006; received in revised form 23 February 2007; accepted 28 February 2007

Abstract

Using the well-known Regional Atmospheric Modelling System (RAMS) version 4.3 an integrated system able to simulate the atmospheric mercury cycle has been developed. Basic processes of the mercury atmospheric cycle have been incorporated into the atmospheric model. The model deals with elemental Hg (Hg^0), divalent gaseous Hg (Hg^2) and particulate Hg (Hg^P). Wet deposition mechanisms used to describe the removal of Hg^2 and Hg^P are merged with the detailed cloud microphysical scheme in order to provide better representation of the wet deposition processes. The advantages of this approach have been examined through results intercomparison with simulated Hg wet deposition using CMAQ-Hg from previous work for two evaluation periods: 4 April–2 May 1995, and 20 June–18 July 1995. An attempt to clarify the main parameters that affect wet deposition mechanism of mercury is also made.

Keywords: Atmospheric mercury; Modelling system; Evaluation; Model coupling intercomparison

1. Introduction

Mercury is a multi-scale pollutant able to be transmitted at local, regional and long scale distances from the sources following the various physico-chemical properties, of the three species examined. Elemental mercury (Hg^0) is known having an atmospheric residence time of 0.5–2 years, divalent gaseous mercury (Hg^2) remains in the atmosphere for a few hours or days, while for particulate mercury (Hg^P) residence time is a few weeks (Lindqvist and Rodhe, 1985; Schroeder and Munthe, 1998). Over the past years several studies have been conducted to describe the behaviour of mercury released into the atmosphere using mathematical models (Pai et al., 1997; Petersen et al., 1998; Xu et al., 2000; Seigneur et al., 2001; Travnikov and Ryaboshapko, 2002).

RAMS-Hg and CMAQ-Hg are two state-of-the-science integrated modelling systems developed to study the complex chemical transformation, transport and deposition of atmospheric mercury. CMAQ-Hg is an expanded version of the US EPA's Community Multiscale Air Quality, CMAQ model (Byun and Ching, 1999) modified accordingly by Bullock and Brehme (2002), referred hereafter as BB, to simulate the atmospheric cycle of mercury. In CMAQ-Hg, a detailed physio-chemical

*Corresponding author. Tel.: +30 210 7276835; fax: +30 210 7276765.
E-mail address: kallos@mg.uoa.gr (G. Kallos).

1352-2310/$ - see front matter
doi:10.1016/j.atmosenv.2007.02.045

mechanism of Hg, involving both gaseous and aqueous phases is included to provide an accurate description of the three mercury species. CMAQ-Hg uses meteorological inputs from the mesoscale model MM5 (Grell et al., 1994). Cloud-water concentrations of the three species, necessary for aqueous phase chemistry and wet deposition estimated in CMAQ-Hg are based on the calculation from the MM5 meteorological model simulation (Bullock and Brehme, 2002). However, many other meteorological processes are important for the transformation and deposition of mercury and need to be considered at each time loop. For example, good representation of turbulence is important for dry deposition of mercury, while wet deposited amount of the mercury species considered, is strongly dependent on the microphysical scheme adapted by the meteorological model.

In most of the conventional models used to simulate the atmospheric mercury cycle, precipitation is poorly represented leading to non-accurate calculations of wet deposition of mercury. RAMS-Hg is developed using one of the most advanced atmospheric modelling systems available today, namely RAMS (Cotton et al., 2003). In RAMS-Hg, basic processes like advection and diffusion already existing in the atmospheric model for passive tracers have been modified accordingly for mercury species. Other processes to describe mechanisms such as chemical transformations, wet and dry deposition and air-surface exchange of mercury have been developed and incorporated in the full-physics meteorological model RAMS.

The main objective of the present work is to identify advantages related to the direct coupling of meteorology to mercury-oriented processes. The benefits/costs associated with the proposed approach are examined through the comparison of model results with both observations from the Hg deposition network (MDN) and wet deposition of Hg results using CMAQ-Hg from the previous work of BB. The dependence on accurate precipitation calculations pointed out by BB, as well as the advantages of model coupling are examined in this study, for two experimental periods, namely 4 April–5 May 1995 and 20 June–18 July 1995. Researchers using statistical measures, such as BIAS, percentiles, the Pearson correlation coefficient of modelling results to actual observations of wet deposition and precipitation, showed that the performance of the model on calculating wet deposition of mercury is strongly depended on the correlation between observed and modelled precipitation.

The modelling system was applied to a domain covering most of eastern North America. A preliminary validation of the RAMS-Hg model as well as quantitative estimation of the advantages of the proposed approach on coupling mercury processes to an atmospheric modelling system are presented.

2. Model description and setup

The developed integrated RAMS-Hg modelling system includes the various atmospheric and surface processes of mercury species that describe the atmospheric mercury cycle. These basic features of the model are briefly described below:

Anthropogenic emissions: The mercury emissions released from anthropogenic sources are considered through the inclusion of each mercury emission inventory available for the simulation area and period. The various sources (e.g. power plants, waste incinerators, coal combustion) are automatically allocated within the model domain according to the geographic co-ordinates and the type of sources (area and point sources).

Natural emissions– re-emissions-atmosphere-surface exchange: Both natural emissions and re-emissions are considered in the developed model and treated accordingly. Fluxes of mercury from soil and water had been considered constant at previous version of the model. Mercury fluxes from soil are now calculated as a function of soil temperature (Capri and Lindberg, 1998; Xu et al., 1999), while for air–water exchange of mercury, wind speed at 10 m above surface, whitecap coverage, friction velocity and Hg^0 concentration in air and water are considered (Mackay and Yeun, 1983; Shannon and Voldner, 1995; Xu et al., 1999).

Chemistry module: The chemistry module includes 107 reactions and deals not only with the gas and aqueous phase chemistry reactions of mercury species with other reactants, but also with photochemical, bimolecular and termolecular reactions that form these reactants. The photochemical reactions of ozone (O_3) and hydrogen peroxide (H_2O_2) both in aqueous and gaseous phases are treated within the chemistry module using the Fast-J scheme proposed by Wild et al. (2000). Other reactions include the bimolecular reactions of SO_x, CO and CO_2 with O_2, H_2O, OH and H_2O_2. Sommar et al. (2001) correction on the rate constant of the gas phase reaction between Hg^0 and OH has been adopted. The gas and liquid phase reactions of mercury considered in the chemistry module are those with O_3, H_2O_2, chlorines and sulphite (Munthe et al., 1991; Munthe, 1992). It should be noted that the gaseous and aqueous phase chemistry mercury reactions are similar to the ones adopted by BB. One of the benefits of the chemistry module incorporated in RAMS is its flexibility, the ability to calculate online the rate constants of the reactions for various temperatures, pressures and water content as well as the simplicity to add new reactions to the database.

Dry deposition module: In most deposition models the deposited quantity over a given surface is the product of the pollutant's concentration at the first model level (close to the surface) and the deposition velocity. In the dry deposition process the velocity is calculated using the resistance method. Using this method, deposition is calculated as the sum of various resistances for the gaseous species (Hicks et al., 1985) and the settling velocity for particles. The values of the resistances depend upon meteorological conditions as well as on the properties of the surface. The deposition velocity for Hg^0 is not considered. The deposition velocity of Hg associated with particles, (Hg^P), was calculated by distributing its mass according to a lognormal particle size distribution. The whole particle size distribution is subdivided into 15 size intervals and the deposition velocity is calculated for each interval. Thus the deposition velocity of Hg^P is obtained as a weighted average of the previous velocities. The deposition velocities calculated for Hg^2 and Hg^P are close to the ones considered by Pai et al. (1997) and Shannon and Voldner (1995). The range of the deposition velocities is 0.1–1 $cm\,s^{-1}$ for Hg^2 and 0.02–0.2 $cm\,s^{-1}$ for Hg^P.

Wet deposition module: The wet removal process concerns the soluble chemical species (Hg^2 and its compounds), and also the particulate matter (Hg^P) scavenged only from below the precipitating clouds. Wet scavenging of the divalent mercury (Hg^2) is assumed to occur in and below clouds. As Hg^2 has similar aqueous solubility with HNO_3 (Xu et al., 2000), it is assumed to be an irreversibly soluble gas and its scavenging coefficient is calculated accordingly (Seinfeld and Pandis, 1998). In cloud, Hg^2 can be removed by interstitial cloud air by dissolution into cloud drops. The local rate of removal of the irreversibly soluble gas with a concentration depends on the scavenging coefficient of the gas in the cloud and on the concentration of the pollutant.

This integrated RAMS-Hg modelling system has been applied for two periods, the spring (4 April 1995–2 May 1995) and the summer (20 June–18 July 1995) simulation period, also discussed in the study of BB in an attempt to repeat their study and compare model results with the published ones. The domain of both simulations covers the area of US East of the Rocky Mountains, with 36 km horizontal grid increment also used in the study of BB, as shown in Fig. 1 and 30 vertical levels, reaching up to 50 hPa. Other data such as vegetation and topography extracted from USGS (United States Geophysical Survey) are similar to the ones used for MM5 meteorological simulation.

Meteorological data: The model was initialized with gridded data sets containing horizontal velocity components, temperature, geopotential height and relative humidity as a function of pressure. More specifically, the data were obtained from the European Center for Medium Range Forecasting (ECMWF). Their horizontal increment is 0.5°, and they were available every 6 h (0000, 0600, 1200 and 1800 UTC).

Emission data: The New York State Department of Environmental Conservation provided the emission data used in both simulations (spring and summer). This mercury emission inventory includes all categories of sources (area, point sources). The emission data include information for each point source, such as the location of the source, latitude and longitude, stack height, information on the emission type (Hg^0, Hg^2 and Hg^P) and type of plant. The final processing of this inventory was performed and described in Walcek et al. (2003), while the same inventory has been also used in previous work of Voudouri et al. (2005). Mercury emissions extracted from the Global Mercury Emission Inventory have been used also for the rest of the computational domain. These emission data are close to the ones used in the BB study. Thus all anthropogenic and natural sources and source categories included are comparable, in an attempt to homogenize the performed simulations with the ones presented by BB.

Initial and boundary conditions for Hg^0, Hg^2 and Hg^P: Horizontally homogeneous initial and boundary conditions were used for the three mercury species similar to the ones used by BB and Lin and Tao (2003). The lateral boundary concentrations of all species were fixed throughout the simulations.

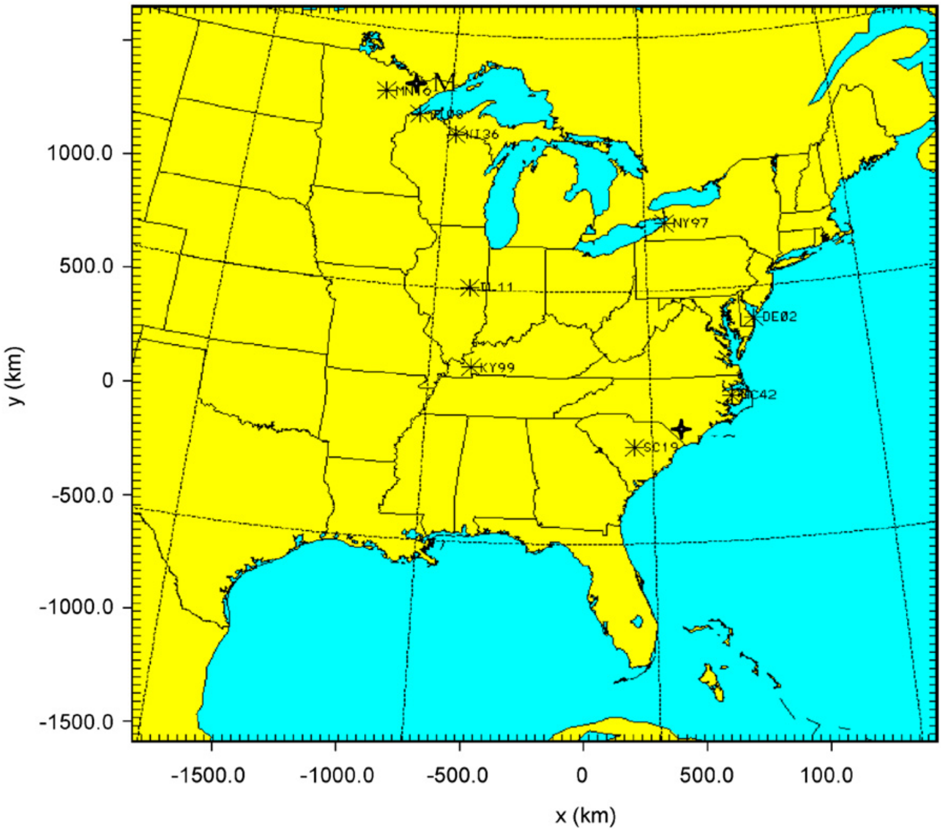

Fig. 1. The model domain and the MDN site locations used to evaluate the model performance.

Initial and lateral boundary concentrations of $1.6\,ng\,m^{-3}$, 10 and $10\,pg\,m^{-3}$ were used for Hg^0, Hg^2 and Hg^P, respectively, in the lowest model level. The initial and lateral boundary concentrations of the three species were assumed to decrease with height. Measurements of stratospheric aerosol particles showed that mercury can also be found at altitudes up to 19 km (Murphy et al., 1998). Therefore all three species decrease with height following a tangent hyperbolic profile, reaching $0.02\,ng\,m^{-3}$ for Hg^0 and $0.08\,pg\,m^{-3}$ for Hg^2 and Hg^P in the upper model level. It should also be noted that results are in general worst when using a model as a stand-alone system, instead of feeding lateral boundary conditions from a global scale model. It should be added that researchers' indention was to perform the worst case scenario by using the same initial and boundary conditions.

Wet deposition data used for model validation, are the ones also used by BB for both spring and summer simulation period. These data correspond to 11 MDN stations for summer; while for spring only eight stations reported (two stations in North Carolina and one in Wisconsin were not operating at the time). More specifically the stations used for both simulation periods are presented in Table 1 (also shown in Fig. 1). Its station provided weekly measured wet deposited Hg, namely 28 samples for spring and 35 samples for summer simulation period.

3. Model runs, analysis of results

RAMS-Hg model has been applied for the spring and summer period and results have been compared with wet deposition and precipitation observations available for both simulation periods from MDN. Observed precipitation was derived from wet deposition ($ng\,m^{-3}$) and sample concentration ($ng\,lt^{-1}$) data. Precipitation is the key parameter for wet deposited Hg, therefore observations have been also compared with precipitation amounts calculated using RAMS-Hg. Comparison of model results for precipitation versus observations for the spring season period are presented in Table 2, while observed and modelled wet deposited Hg values are presented in Table 3, respectively. The precipitation observations seem to be in agreement with model results for most stations during the spring simulation period as shown in Table 2. In addition, the

Table 1
Characteristics of MDN stations

Code	Station name	Latitude	Longitude	Height (m)
DE02	Lewes, DE	38.77	−75.10	2
IL11	Bondville, IL	40.05	−88.37	212
KY99	Mulberry Flat, KY	36.90	−88.01	122
MN16	Marcell Experimental Forest, MN	47.53	−93.47	431
MN18	Superior N.F.–Fernberg, MN	47.95	−91.50	524
NC08	Waccamaw State Park, NC	34.17	−78.42	10
NC42	Pettigrew State Park, NC	35.75	−76.37	2
NY97	Sturgeon Point, NY	42.68	−79.03	176
SC19	Congaree Swamp, SC	33.81	−80.78	145
WI08	Brule River, WI	46.75	−91.61	207
WI36	Trout Lake, WI	46.05	−89.65	501

Table 2
Comparison of modelled weekly precipitation (mm) with measurements from 11 MDN sites

Station	MDN 4–11/04/95	RAMS-Hg	MDN 11–18/04/95	RAMS-Hg	MDN 18–25/04/95	RAMS-Hg	MDN 25–02/05/95	RAMS-Hg
DE02	1.94	11.95	23.69	2.69	21.97	17.13	21.57	10.03
IL11			60.78	55.15	16.04	25.66		
KY99	0.00	5.14	1.31	20.18	62.34	30.17	57.69	47.06
MN16	4.58	1.48	25.74	17.24	25.71	19.72	0.00	0.01
MN18	3.89	2.91	22.01	14.75	6.00	16.79	0.00	0.00
NC08								
NC42								
NY97	8.43	9.19	9.90	28.42	4.24	10.39	4.33	4.50
SC19	5.02	9.20	2.04	4.90	7.31	33.42	4.16	19.55
WI08	6.17	2.22			45.24[a]	54.37		
WI36								

[a]Measurement for this station stands for 11–25/04/95.

Table 3
Comparison of modeled weekly wet deposited Hg (ng m^{-2}) with measurements from 11 MDN sites

Station	MDN 4–11/04/95	RAMS-Hg	MDN 11–18/04/95	RAMS-Hg	MDN 18–25/04/95	RAMS-Hg	MDN 25–02/05/95	RAMS-Hg
DE02	98	157.40	118	27.15	248	381.57	275	160.39
IL11			905	498.38	175	129.92		
KY99	0	0.94	23	164.52	773	281.52	484	415.70
MN16	32	57.71	87	141.64	27	183.90	0	1.56
MN18	22	33.56	70	137.99	35	194.90	0	0.00
NC08								
NC42								
NY97	66	182.59	151	296.72	70	90.72	46	121.56
SC19	80	119.10	8	29.68	105	214.77	39	79.05
WI08	40	87.20			228[a]	539.51		
WI36								

[a]Measurement for this station stands for 11–25/04/95.

comparison of weekly observed wet deposition of Hg versus model results for the same period, presented in Table 3, confirms the dependence of wet deposition mechanism on precipitation. Table 3 also indicates that agreement between observed and modelled wet deposited Hg is present during the week 25 April–2 May. This is also the case for modelled and observed precipitation as shown in Table 2 for the specific week. On the contrary during the second week of the spring simulation period (11–18 April) the atmospheric model underestimated the weekly precipitation for stations KY99 and IL11, leading to the poor agreement presented between wet deposition estimations and observations. These specific stations located at Kentucky and Illinois, respectively, were within the warm sector of a depression formed on April 11, as shown in Fig. 2. These stations were also affected by a warm front on 15 April and successive depressions passage over the area from 16 to 18 April. RAMS-Hg predicted these depressions, however neither the exact speed nor the location of the depression centre on April 11, were calculated with the necessary accuracy causing a spatial shift on the model predicted precipitation.

The correlation between calculated and observed precipitation and wet deposited Hg has been evaluated through scatter plots for the entire simulation period, presented in Figs. 3 and 4. For the spring period, the Pearson correlation factor is 0.76 for the precipitation and 0.701 for the wet deposition of Hg. These correlation coefficients

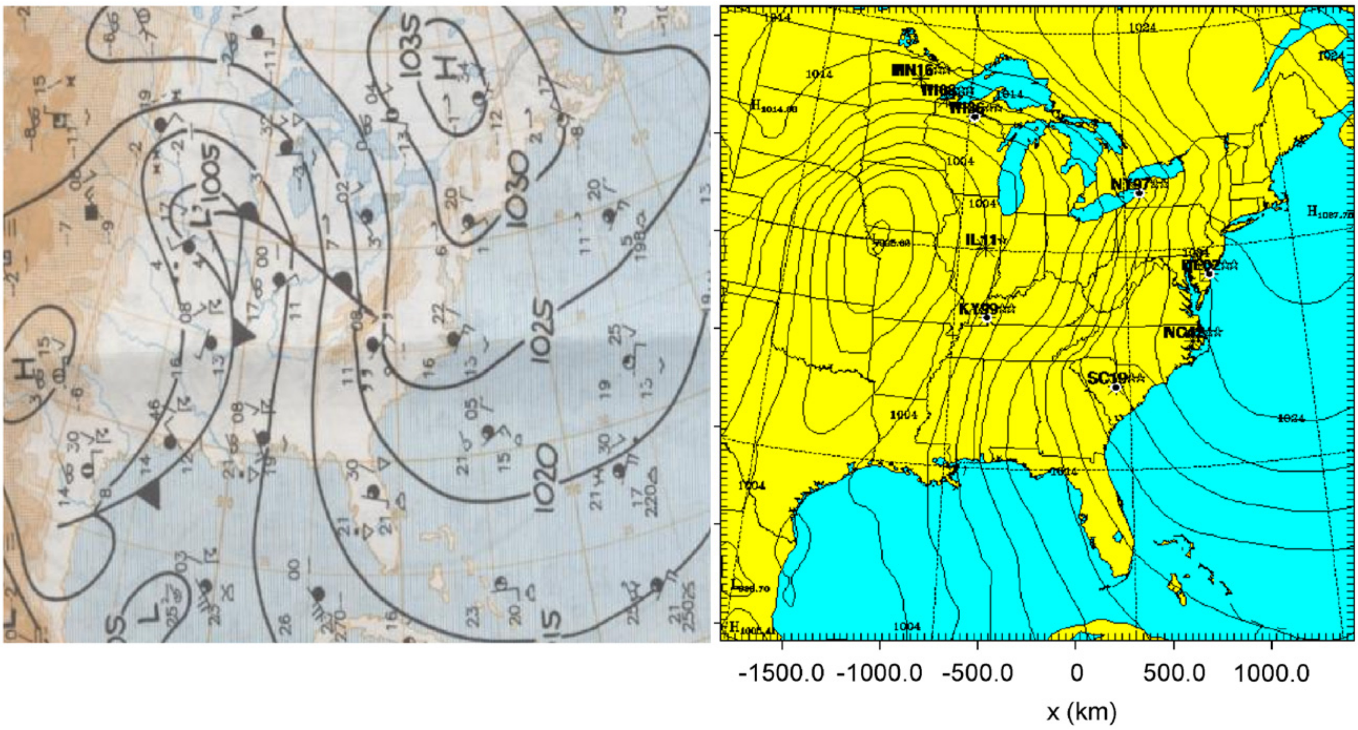

Fig. 2. Surface pressure (mbar) from ECMWF (left panel) and RAMS-Hg (right panel) on 11 April 1995 12 UTC.

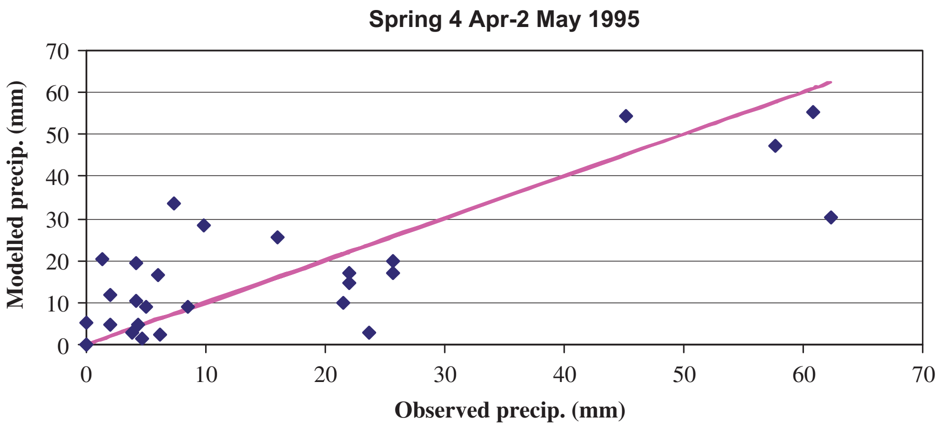

Fig. 3. Scatter plot of total precipitation (mm) during spring experimental period.

indicate relatively good agreement between observations and model calculations with a slight model's tendency to underestimate observed values. This underestimation is more pronounced in cases of heavy precipitation, while in cases where precipitation and wet deposited Hg are less than 10 mm and 200 ng m^{-2}, respectively, the model results are fairly well. Maps of accumulated precipitation (in mm) and total wet deposited Hg (ng m^{-2}) during the spring simulation period are illustrated in Figs. 5 and 6, respectively. Higher amounts of wet deposited mercury are mainly predicted over the eastern states of USA. This area was mainly affected by the passage of cold and warm fronts and deep depressions. Main sources of the pollutant are located over the area with the maximum emission rates west of Washington, DC. It is known that wet deposition is affected not only by precipitation characteristic e.g. duration, but also by locations of the source, as well as the type of Hg source (subsequently Hg species).

These three factors define local maxima to a certain degree. It is known for example, that Hg^2

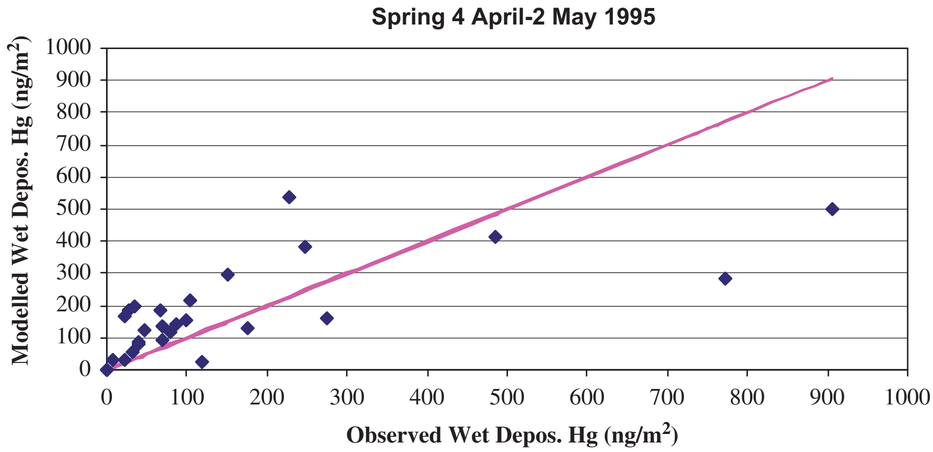

Fig. 4. Scatter plot of wet deposited Hg (ng m^{-2}) during spring experimental period.

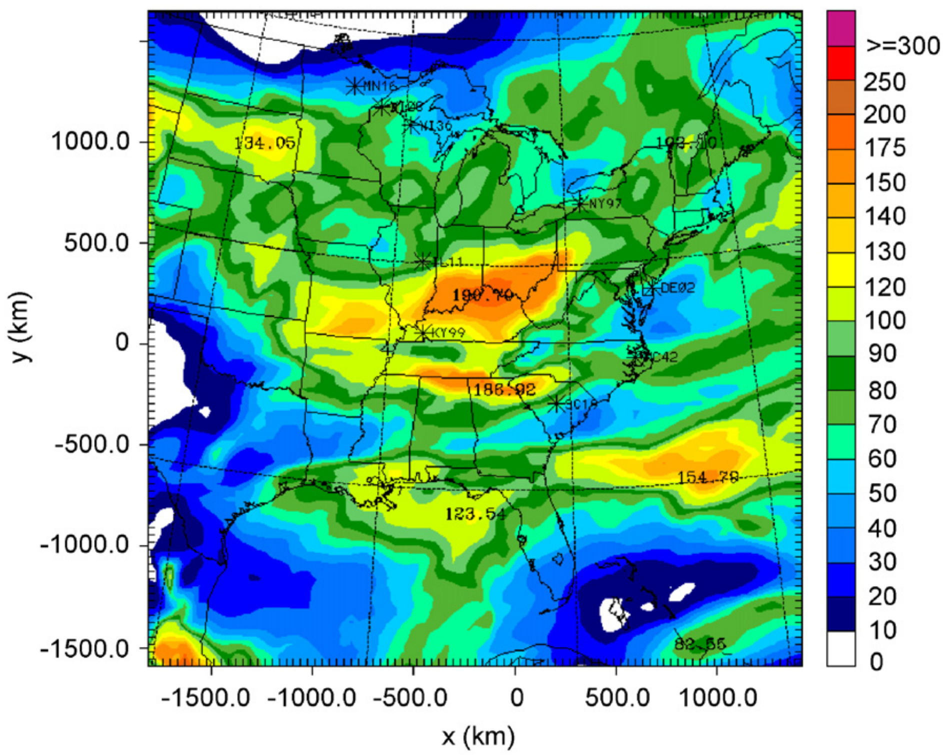

Fig. 5. Accumulated precipitation (in mm) calculated using RAMS-Hg for the spring simulation period.

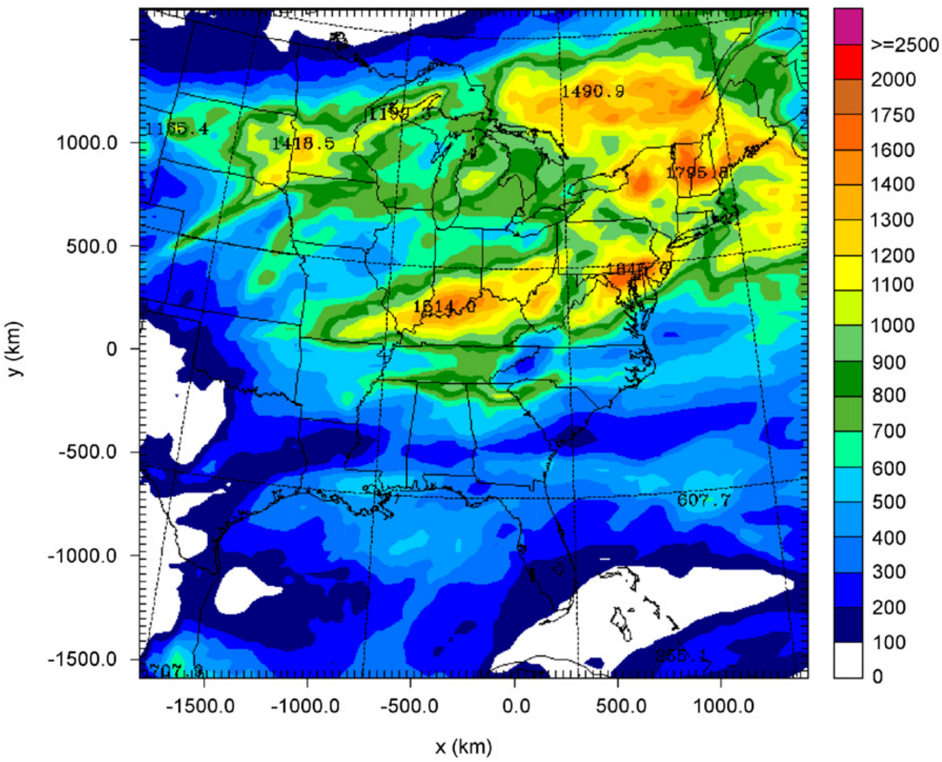

Fig. 6. Total Hg wet deposition (in ng m^{-2}) for the spring simulation period.

and Hg^P dominate the deposition of mercury and are mainly emitted by anthropogenic sources such as power plants, residential heat and waste disposal (Pacyna et al., 2001). Thus, the emission rates are high near Florida; the total precipitation over these areas did not exceed 60 mm, leading to low amounts of wet deposited Hg. On the contrary, local peaks are calculated in the Ohio River valley, while other local peaks are associated with some urbanized areas where high amounts of precipitation are also calculated.

The summer simulation period is associated with the passage of cold fronts over north-eastern and eastern US that favoured the generation of local storms over the area. It should be noted, that the 36 km spatial resolution used for the performed simulations is too coarse to 'capture' such events mainly characterized by strong convective activity and localization of precipitation peaks. Accumulated precipitation and total wet deposited Hg calculated using RAMS-Hg for the entire simulation period are illustrated in Figs. 7 and 8. Accumulated precipitation exceeded 100 mm over the eastern states with local peaks over Florida State. Thus, local peaks of the wet deposited Hg are also calculated during the summer simulation period. Model results compared with available observations from MDN are presented in Table 4, while scatter plot of modelled versus measured wet deposition of Hg is illustrated in Fig. 9.

Inspection of the scatter plot shows that in cases where total wet deposited Hg was less than 300 ng m^{-2}, the model results are in agreement with observations. However, in cases where total amount of wet deposited Hg was greater than 500 ng m^{-2}, the model underestimated the wet deposited amount. This is the case during the last week of the summer simulation period, namely 11–18 July 1995. In addition, the Pearson correlation coefficient for this period was only 0.396, suggesting poor correlation between observations and model results.

Precipitation is known to be the controlling factor for wet deposition. Therefore, an attempt was made to investigate this poor agreement between observations and model calculations of wet deposited Hg for the summer simulation period. Model calculated precipitation has been also compared with the observations. The Pearson correlation coefficient between modelled and observed precipitation is 0.161, indicating low correlation between modelled and observed values. A much wider scatter is evident for precipitation in Fig. 10 during this

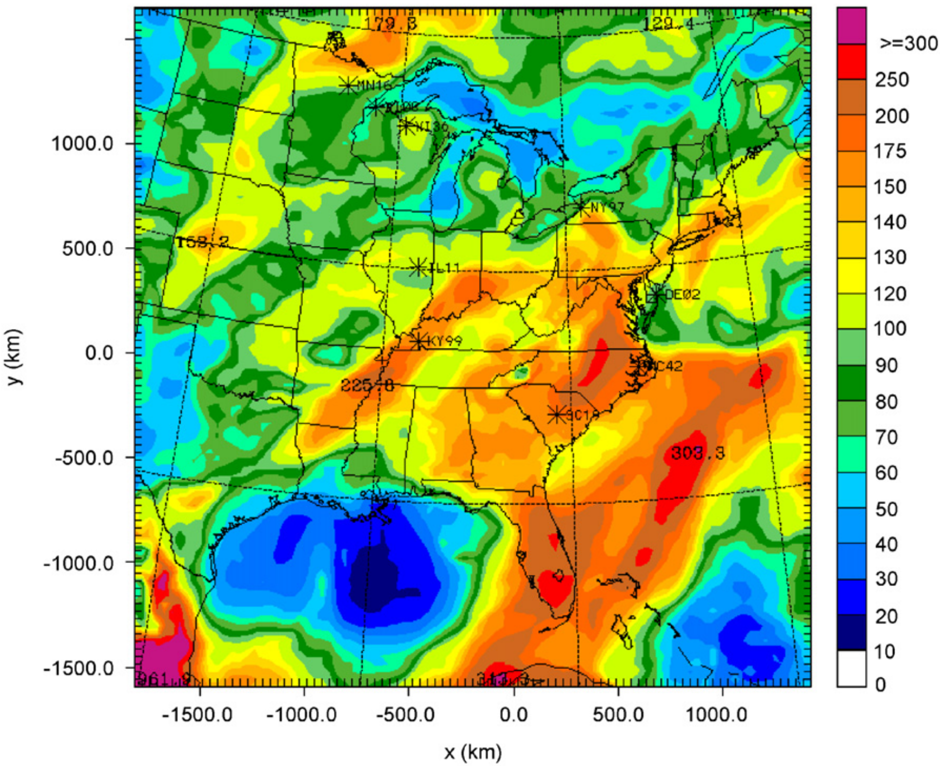

Fig. 7. Accumulated precipitation (mm) calculated using RAMS-Hg for the summer simulation period.

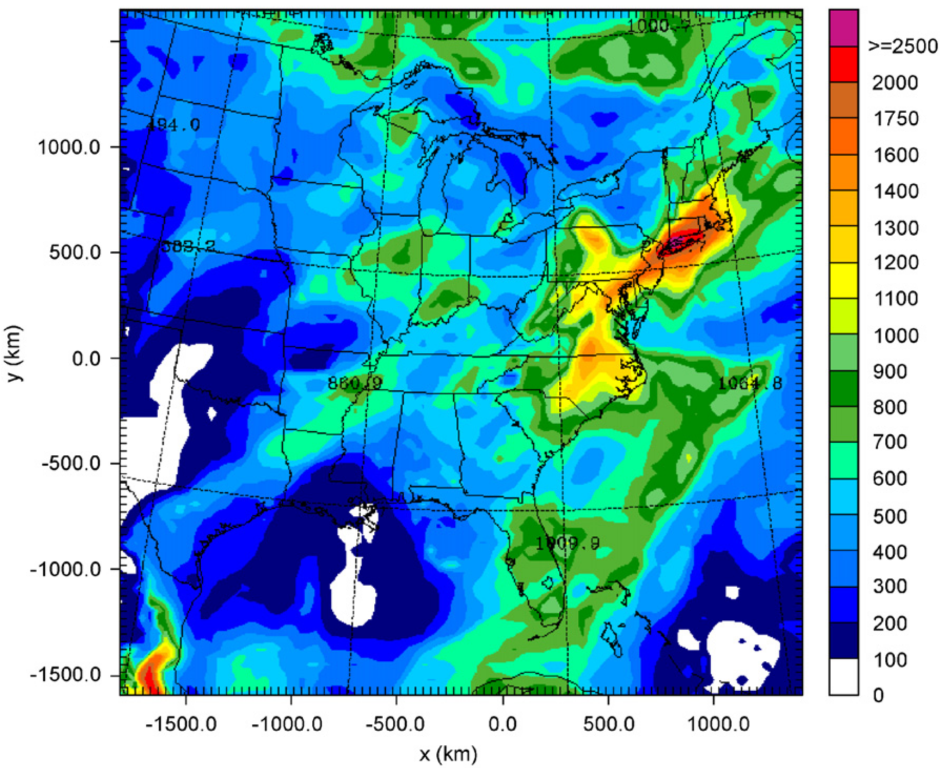

Fig. 8. Total Hg wet deposition (in ng m^{-2}) for the summer simulation period.

simulation period suggesting that the atmospheric model could not adequately represent the prevailing meteorological conditions at the time. This is mainly attributed to the spatial resolution used (same as the one selected by BB), as well as in the local scale of the precipitation events during the simulation

Table 4
Comparison of modelled weekly wet deposited Hg (ng m^{-2}) with measurements from 11 MDN sites

Station	MDN 20–27/06/95	RAMS-Hg	MDN 27–4/07/95	RAMS-Hg	MDN 4–11/07/95	RAMS-Hg	MDN 11–18/07/95	RAMS-Hg
DE02	40	7.77	646	131.07	0	274.16	358	315.77
IL11			95	192.59				
KY99	36	205.55	425	249.28	533	141.58	0	48.23
MN16	378	47.60	222	267.76	371	125.18		
MN18			347	316.28	182	114.61		
NC08	130	280.73	286	286.39	548	226.96	574	59.26
NC42	1207[a]	503.97			493[b]	354.30		
NY97	761	92.07	16	238.78	650	6.85	693	186.48
SC19	972	501.27	250	125.80	697	99.17	210	119.85
WI08	61	102.69	383	184.19	207	65.45		
WI36	234	141.04	0	194.10	227	28.38	1293	329.97

[a]Sample dates 22 June 1995–29 June 1995.
[b]Sample dates 06 July 1995–13 July 1995.

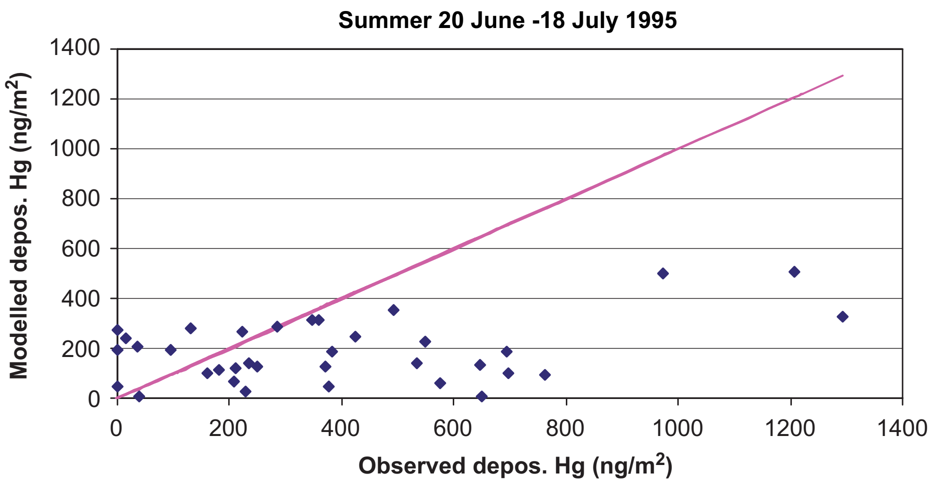

Fig. 9. Scatter plot of wet deposited Hg (in ng m^{-2}) for summer simulation period.

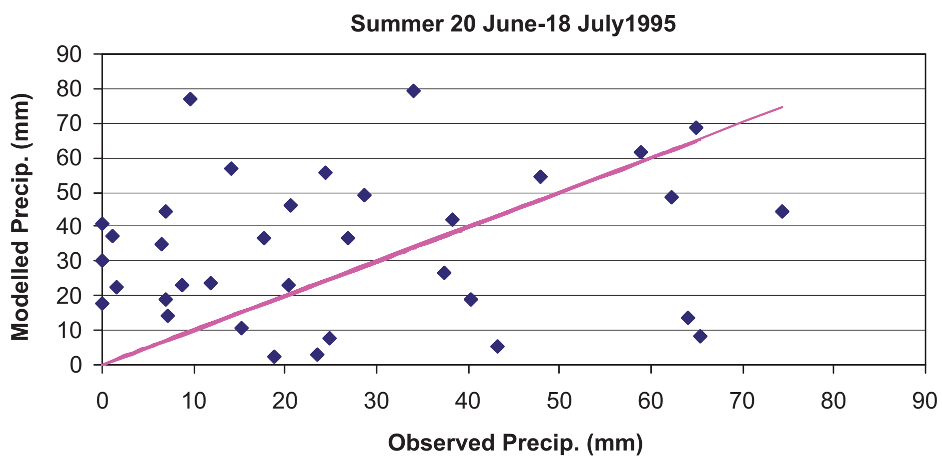

Fig. 10. Scatter plot of precipitation (mm) during the summer simulation period.

period. The selection of the same spatial resolution in the present work was made in order to compare RAMS-Hg performance against CMAQ-Hg used by BB. However, the 36 km spatial resolution is not adequate to describe summer convective activities over NE US. This was also reported in BB.

4. Discussion

A preliminary evaluation of the proposed approach as well as differences between RAMS-Hg and CMAQ-Hg is performed through a comparison of statistics. Model predictions of weekly precipitation and wet deposited Hg using both CMAQ-Hg and RAMS-Hg are compared with weekly measurements made by MDN. Summary statistics of the comparative evaluation between observed and model using RAMS-Hg as well as published data from BB are shown in Tables 5 and 6 for precipitation and wet deposited Hg, respectively.

An improvement is evident for both simulation periods using RAMS-Hg mainly on precipitation and wet deposition of Hg during spring. More specifically, the average value of modelled wet deposited Hg is 168.9 ng m^{-2} compared to the observed 150.2 ng m^{-2} indicating that the model overestimated the wet deposited Hg. The statistics for the summer period indicate that RAMS-Hg underestimated the wet deposition of Hg, reflected in all four quartiles while precipitation is slightly overestimated. However, the weak relationship between observed and modelled precipitation as well as wet deposited Hg inhibits from any conclusion on model reliability for the summer simulation period. Lin and Tao (2003) have also calculated accumulated wet deposited Hg for the

Table 5
Summary statistics for precipitation in mm

Period	N	Source	Average	σ	Min	Percentiles			Max
						25th	50th	75th	
Spring	28	MDN	16.14	18.9	0	4.1	6.7	22.4	62.3
		CMAQ-Hg	10.88	13.37	0	1.9	5.7	17.1	51.5
		RAMS-Hg	18.91	15.58	0	4.8	13.4	21.5	55.2
Summer	35	MDN	26.5	22.01	0	7.975	20.64	39.3	74.31
		CMAQ-Hg	34.4	35.78	0	3.57	16.81	36.31	162.90
		RAMS-Hg	33.8	20.99	2.39	18.32	34.91	47.39	79.39
Spring and summer	63	MDN	21.88	21.17	0	6.53	16.04	31.32	74.31
		CMAQ-Hg	23.97	30.32	0	3.57	16.81	36.31	162.90
		RAMS-Hg	26.34	20.31	0	9.62	20.18	41.65	79.39

Table 6
Summary statistics for wet deposition of Hg in ng m^{-2}

Period	N	Source	Average	σ	Min	Percentiles			Max
						25th	50th	75th	
Spring	28	MDN	150.17	222.3	0	31	70	157	905
		CMAQ-Hg	189.1	232.0	0	21.6	103.1	268.6	843.5
		RAMS-Hg	168.92	145.0	0	73.7	139.82	199.87	539.51
Summer	35	MDN	389.3	327.3	0	171.5	347	561	1293
		CMAQ-Hg	623.7	621.1	0	202.1	482.5	759.7	2598.5
		RAMS-Hg	187.6	124.9	6.85	100.9	184.19	270.96	503.96
		Lin and Tao	409.6	318.9	0	192.2	388.2	583.5	1143.9
Spring and summer	63	MDN	283.0	307.6	0	65.59	182	404	1293
		CMAQ-Hg	430.5	531.4	0	82.50	247.10	576.30	2598.50
		RAMS-Hg	179.3	132.37	0	88.96	141.64	258.52	539.51

entire summer experimental period as shown in Table 6. These researchers have used CMAQ-Hg with meteorological data generated from MM5 simulations. Although these results indicate a slightly improvement against the previous work of BB, they are not considered in the RAMS-Hg evaluation. Despite the fact that they have used the same spatial resolution, leading to the poor performance of MM5 on precipitation, surprisingly, their Hg wet deposition calculations are in very good agreement with the observations. The researchers attributed it to the reduced rate constant of the gaseous oxidation of Hg^0 by OH. They did not perform the same evaluation for the spring simulation period.

Additional comparisons of statistics are summarized in Table 7. The calculated correlation coefficient between modelled and observed wet deposited Hg for the eight stations operating during the spring simulation period is 0.701, indicating a slightly improvement over the correlation coefficient 0.657 calculated by BB. BIAS of modelled wet deposited Hg using RAMS-Hg is equal to 18.75 $ng\,m^{-2}$ compared to 38.93 $ng\,m^{-2}$ BIAS for CMAQ-Hg for spring simulation period. During the summer simulation period, the CMAQ-Hg strongly overestimated the measurements as indicated by the positive BIAS of 234.4 $ng\,m^{-2}$ while the RAMS-Hg BIAS is negative -201.7 $ng\,m^{-2}$ suggesting an equally strong underestimation. However, the RAMS-Hg simulation gave improved average values as compared to the calculated by BB ones of wet deposited Hg by 51.8% and 13.9% for spring and summer, respectively. This improvement is mainly attributed to the modelled precipitation and the direct coupling of meteorology with the Hg processes and especially wet deposition.

Combining both simulation period results, in order to increase the sample to 63, it is evident that RAMS-Hg underestimates (BIAS = -103.7 $ng\,m^{-2}$) while CMAQ-Hg overestimates (BIAS = 147.5 $ng\,m^{-2}$) the observations of wet deposited Hg. This BIAS improvement stands for 29.6% for the entire sample (63 measurements for both spring and summer). The implementation of the developed mercury modules on the atmospheric model (direct coupling) in addition to the new developments on the RAMS physics (Cotton et al., 2003) seem to have improved the performance of RAMS-Hg against MM5/CMAQ-Hg indirect coupling approach. This is also pronounced by other statistical figures (such as the ABSBIAS and RMSE of RAMS-Hg equal to 197.2 and 286.9 $ng\,m^{-2}$, respectively) that are not available for CMAQ-Hg results.

The implementation of processes describing mercury transformation and deposition mechanisms in the regional-scale model RAMS could be a useful tool in micro/mesoscale applications such as calculating wet deposition of Hg^2 and Hg^P from local sources. On the contrary, climate-type (or policy-type) of calculations of deposited Hg are also related to Hg^0 concentrations that is a global scale pollutant. Therefore, the proposed RAMS-Hg model development is a useful tool for limited area studies where wet deposition processes (mesoscale precipitation processes) are important. For larger scale studies, the model has the nesting capability by itself for up to hemispheric scales or in a global scale modelling mercury system.

5. Conclusion

In the present study, an application of the developed RAMS-Hg model for two four-week periods in April/May and June/July 1995 was performed. Model validation indicated that the comprehensive model simulated reasonably well the wet deposition measurements of Hg at the MDN sites. Results from both simulations revealed that RAMS-Hg could accurately calculate wet deposited Hg when regional scale meteorological systems prevail. The results of the spring simulation period indicated that the model improved the accuracy on calculated wet deposition of Hg,

Table 7
BIAS (in $ng\,m^{-2}$) and Pearson correlation coefficient for wet deposition of Hg

Measure	Spring		Summer		Spring and summer	
	RAMS-Hg	CMAQ-Hg	RAMS-Hg	CMAQ-Hg	RAMS-Hg	CMAQ-Hg
BIAS	18.75	38.93	−201.7	234.4	−103.7	147.5
Pearson	0.701	0.657	0.396	0.329	0.484	0.474

following the well-defined precipitation pattern. The proposed approach on implementing mechanisms that describe mercury processes into the atmospheric model (direct coupling) reduced limitations or uncertainties derived from poor description of meteorology and reflected mainly on wet and dry deposition treatment. Several concerns remain on the accuracy of the MDN measurements, due to lack of valid measurements by all stations used in the present study. Considering the rather small sample size, model results are encouraging. The proposed approach seems to be more appropriate for inducing micro/mesoscale policy strategies due to better representation of the physico-chemical processes occurred in these scales. Although, the RAMS-Hg modelling system can be configured to run for up to hemispheric base as stand-alone or nested within a global system. This comprehensive regional modelling study was performed by including the up to date physio-chemical transformation mechanism of Hg, however further development on Hg re-emission treatment, dry deposition and model validation is planned based on the results of this study.

Acknowledgements

This work was performed at the framework of the MERCYMS ('An Integrated Approach to Assess the Mercury Cycling in the Mediterranean Basin') project funded by EU DG-Research, contract EVK3-2002-00070. R. Bullock is acknowledged for useful information exchange, as well as the MDN for making the deposition data available.

References

Bullock Jr., O.R., Brehme, K.A., 2002. Atmospheric mercury simulation using the CMAQ model: formulation description and analysis of wet deposition results. Atmospheric Environment 36, 2135–2146.

Byun, D. W., Ching, J. K. S., 1999. Science Algorithms of the EPA Models-3 Community Multiscale Air Quality (CMAQ) Modeling System, EPA/600/R-99/030. Environmental Protection Agency, Office of Research and Development, Washington, DC.

Capri, A., Lindberg, S.E., 1998. Application of a Teflon dynamic flux chamber for quantifying soil mercury flux: tests and results over background soil. Atmospheric Environment 32, 873–882.

Cotton, W.R., Pielke, R.A., Walko, R.L., Liston, G.E., Tremback, C.J., Jiang, H., McAnelly, R.L., Harrington, J.Y., Nicholls, M.E., Carrio, G.G., McFadden, J.P., 2003. RAMS 2001: current status and future directions. Meteorology and Atmospheric Physics 82, 5–29.

Grell, G. A., Dudhia, J., Stauffer, D. R., 1994. A description of the fifth-generation Penn State/NCAR mesoscale model (MM5). NCAR Technical Note, NCAR/TN-398 + STR.

Hicks, B. B., Baldocchi, D. D., Hosker Jr., R.P., Hutchison, B. A., Matt, D. R., McMillen, R. T., Satterfield, L. C., 1985. On the use of monitored air concentrations to infer Dry Deposition. NOAA Technical Memorandum ERL ARL-141, Silver Spring, MD.

Lin, X., Tao, Y., 2003. A numerical study on regional mercury budget for eastern North America. Atmospheric Chemistry and Physics 3, 535–548.

Lindqvist, O., Rodhe, H., 1985. Atmospheric mercury-a review. Tellus 27B, 136–159.

Mackay, D., Yeun, A.T.K., 1983. Mass transfer coefficient correlations for volatilization of organic solutes from water. Environmental Science and Technology 17, 211–217.

Munthe, J., 1992. The aqueous oxidation of elemental mercury by ozone. Atmospheric Environment Part A—General Topics 26 (8), 1461–1468.

Munthe, J., Xiao, Z.F., Lindqvist, O., 1991. The aqueous reduction of divalent mercury by sulfite. Water Air and Soil Pollution 56, 621–630.

Murphy, D.M., Thompson, D.S., Mahoney, M.J., 1998. In situ measurements of organics, meteoritic material, mercury, and other elements in aerosols at 5 to 19 kilometers. Science 282, 1664–1669.

Pacyna, E.G., Pacyna, J.M., Pirrone, N., 2001. European emissions of atmospheric mercury from anthropogenic sources in 1995. Atmospheric Environment 35, 2987–2996.

Pai, P., Karamchandani, P., Seigneur, C., 1997. Simulation of the regional atmospheric transport and fate of mercury using a comprehensive Eulerian model. Atmospheric Environment 31, 2717–2732.

Petersen, G., Munthe, J., Pleijel, K., Bloxam, R., Kumar, A.V., 1998. A comprehensive Eulerian modelling framework for airborne mercury species: development and testing of the tropospheric chemistry module (TCM). Atmospheric Environment 32, 829–843.

Schroeder, W., Munthe, J., 1998. Atmospheric mercury—an overview. Atmospheric Environment 32, 809–822.

Seigneur, C., Karamchandani, P., Lohman, K., Vijayaraghavan, K., Shia, R.-L., 2001. Multiscale modeling of the atmospheric fate and transport of mercury. Journal of Geophysical Research 106 (D21), 27795–27809.

Seinfeld, J.H., Pandis, S.N., 1998. Atmospheric Chemistry and Physics. From Air Pollution to Climate Change. Wiley, New York, NY.

Shannon, J.D., Voldner, E.C., 1995. Modeling atmospheric concentrations of mercury and deposition to the Great Lakes. Atmospheric Environment 29, 1649–1661.

Sommar, J., Gardfeldt, K., Stromberg, D., Feng, X.B., 2001. A kinetic study of the gas-phase reaction between the hydroxyl radical and atomic mercury. Atmospheric Environment 35, 3049–3054.

Travnikov, O., Ryaboshapko, A., 2002. Modeling of mercury hemispheric transport and depositions. EMEP/MSC-E Technical Report 6/2002, 67pp.

Voudouri, A., Pytharoulis, I., Kallos, G., 2005. Mercury budget estimates for the State of New York. Environmental Fluid Mechanics 5, 87–107.

Walcek, C., De Santis, S., Gentile, T., 2003. Preparation of mercury emissions inventory for eastern North America. Environmental Pollution 123, 375–381.

Wild, O., Zhu, X., Prather, M., 2000. Fast-J: accurate simulation of in- and below-cloud photolysis in the tropospheric chemical models. Journal of Atmospheric Chemistry 37, 245–282.

Xu, X., Yang., X., Miller, D.R., Helble, J.J., Carley, R.J., 1999. Formulation of bi-directional atmosphere-surface exchanges of elemental mercury. Atmospheric Environment 33, 4345–4355.

Xu, X., Yang, X., Miller, D.R., Helble, J.J., Carley, R.J., 2000. A regional scale modeling study of atmospheric transport and transformation of mercury. I. Model development and evaluation. Atmospheric Environment 34 (28), 4933–4944.